Gulf Journal of Mathematics ISSN: 2309-4966
Vol 22, Issue 1 (2026) 1-12 https://doi.org/10.56947/gjom.v22i1.3819

A NEW CUBIC GENERALIZED HERMITE SPLINE INTERPOLATION

CHAIMAE MOUHOUB[1*] and MOHAMED-YASSIR NOUR[2]

Abstract. This work introduces an original interpolation approach for cubic Hermite splines constructed within a generalized spline framework. The proposed technique simultaneously approximates the function and its first-order derivatives. Several numerical experiments are presented, highlighting the accuracy and effectiveness of the method.

Keywords. Generalized spline constructions, Hermite-type interpolation, derivative-based optimization.
2020 Mathematics Subject Classification. Primary 65D07, 65N30, 41A15; Secondary 35K20, 46L55.

1. Introduction

Over the past few decades, significant advances in numerical approximation have been achieved, largely influenced by improved understanding of geometric smoothness and by the introduction of broader classes of functional spaces (see, for instance, [9, 12] and the references therein).

Among the earlier works, H. Akima [1] introduced a method for smooth curve construction using piecewise-defined representations, where the local behavior at interpolation points is governed by geometrically motivated slope estimates. Subsequently, K. Ichida and coauthors [8] employed cubic Hermite splines to develop a least-squares fitting strategy that, while not fully optimal, demonstrated strong practical performance. In a related direction, A. M. Bica et al. [4] proved an optimality result for cubic splines of Hermite type and illustrated its effectiveness in approximation problems. More recently, X. Han et al. [7] proposed a cubic Hermite interpolation framework in which nodal derivatives are determined through an optimization process within the spline space. Consider a subdivision $a = x_1 < \cdots < x_n = b$ of the interval $I := [a, b]$, whose total length is bounded by 2π. Assume that function values y_i and derivative data m_i are given at the nodes for $i = 1, \ldots, n$. It is a classical result that, on each subinterval $[x_i, x_{i+1}]$,

Date: Received: Nov 11, 2025; Revised: Dec 9, 2025; Accepted: Dec 21, 2026.
* Corresponding author

there exists a unique polynomial $H_i \in \mathbb{P}_3$ such that

$$H_i(x_i) = y_i, \qquad H_i(x_{i+1}) = y_{i+1},$$

$$H_i'(x_i) = m_i, \qquad H_i'(x_{i+1}) = m_{i+1}.$$

By assembling these local polynomials, one obtains a piecewise cubic function H of class $\mathcal{C}^1$ on I, which interpolates the data (x_i, y_i) while matching the prescribed nodal derivatives.

In practical situations, the values y_i are usually known, whereas the derivatives m_i at the nodes must be determined through either local or global procedures. For instance, imposing the additional smoothness requirement $H \in \mathcal{C}^2$ leads to a tridiagonal linear system for the derivative vector $m = (m_1, \ldots, m_n)$ (see [5]). Alternatively, the derivatives may be obtained by minimizing suitable functionals, such as, for $k = 0, 1, 2$,

$$I_k(m) := \int_a^b \left(H^{(k)}(x) - L^{(k)}(x)\right)^2 dx = \sum_{i=1}^{n-1} \int_{x_i}^{x_{i+1}} \left(H_i^{(k)}(x) - L_i^{(k)}(x)\right)^2 dx,$$

where L_i denotes the piecewise linear interpolant defined by

$$L_i(x) := \frac{x_{i+1} - x}{x_{i+1} - x_i} y_i + \frac{x - x_i}{x_{i+1} - x_i} y_{i+1}.$$

This interpolating function represents the most basic construction that preserves the geometric features of the data, although it does not provide a high level of smoothness.

The minimization of the functional I_2 leads to the well-known natural cubic spline. In [4], the authors consider the minimization of I_0, which results in an interpolant characterized by minimal mean-square variation. By contrast, the strategy introduced in [7] relies on minimizing I_1, yielding a set of nodal derivatives m_i such that the resulting spline H exhibits the smallest average discrepancy between its derivative and L'.

Most available interpolation techniques are designed for standard curve families, including conics and clothoids. In the present study, we propose and investigate a novel Hermite-type interpolation scheme. The corresponding operator is constructed to exactly reproduce the functional space generated by $\{1, t, \cos(\omega t), \sin(\omega t)\}$, where $\omega \in \mathbb{R}^+ \cup i\mathbb{R}^+$. An optimal Hermite interpolation procedure, based on the same optimization principle, is also introduced.

Numerical simulations indicate the existence of an optimal choice of the parameter ω, for which the associated quasi-interpolant outperforms several existing approaches [9, 12]. These experiments confirm both the precision and the stability of the proposed Hermite interpolants. An important feature of the generalized formulation is its practical simplicity: all numerical experiments can be carried out within a single computational framework. Only the parameter ω needs to be selected appropriately, eliminating the necessity of developing separate codes for different test problems. With a suitable tuning of this parameter, the overall computational efficiency is significantly enhanced.

The paper is organized as follows. Section 2 presents the construction of the generalized Hermite interpolant, where the nodal derivatives are obtained by solving a suitable minimization problem, and provides an accompanying error analysis. Section 3 is devoted to numerical experiments that illustrate the performance of the proposed method.

2. Generalized Hermite Splines

2.1. **Construction of the Spline.** Consider a uniform subdivision

$$\Delta := \{x_i\}_{1\le i\le n} \subset [a,b], \qquad x_i = a + (i-1)h, \qquad h = \frac{b-a}{n}. \tag{2.1}$$

On each subinterval $[x_i, x_{i+1}]$, suppose that the function values y_i and derivative values m_i are given. Then, there exists a unique generalized Hermite interpolant

$$H_i(x) \in \operatorname{span}\{1, x, \cos(\omega x), \sin(\omega x)\}, \quad \omega \in \mathbb{R}_+ \cup i\mathbb{R}_+, \tag{2.2}$$

which satisfies the Hermite interpolation conditions

$$H_i(x_i) = y_i, \qquad H_i(x_{i+1}) = y_{i+1}, \qquad H_i'(x_i) = m_i, \qquad H_i'(x_{i+1}) = m_{i+1}. \tag{2.3}$$

The global spline $H(x)$, constructed by connecting all the local interpolants H_i, belongs to class $\mathcal{C}^1$ and interpolates the given data (y_i, m_i) [11].

Remark 2.1. The $\mathcal{C}^1$ continuity is ensured provided that the step size h is sufficiently small and that the nodal derivatives m_i satisfy the tridiagonal system presented below.

2.2. **Hermite Basis Functions.** Each local interpolant H_i can be expressed in terms of a Hermite basis as

$$H_i(x) = y_i\phi_{i,1}(x) + y_{i+1}\phi_{i,2}(x) + m_i\phi_{i,3}(x) + m_{i+1}\phi_{i,4}(x), \quad x \in [x_i, x_{i+1}], \tag{2.4}$$

where the basis functions $\phi_{i,j}$, for $j = 1, \dots, 4$, are elements of $\operatorname{span}\{1, x, \cos(\omega x), \sin(\omega x)\}$ and satisfy the Hermite interpolation conditions:

$$\begin{aligned}
\phi_{i,1}(x_i) &= 1, & \phi_{i,2}(x_i) = \phi_{i,3}(x_i) = \phi_{i,4}(x_i) &= 0,\\
\phi_{i,2}(x_{i+1}) &= 1, & \phi_{i,1}(x_{i+1}) = \phi_{i,3}(x_{i+1}) = \phi_{i,4}(x_{i+1}) &= 0,\\
\phi_{i,3}'(x_i) &= 1, & \phi_{i,1}'(x_i) = \phi_{i,2}'(x_i) = \phi_{i,4}'(x_i) &= 0,\\
\phi_{i,4}'(x_{i+1}) &= 1, & \phi_{i,1}'(x_{i+1}) = \phi_{i,2}'(x_{i+1}) = \phi_{i,3}'(x_{i+1}) &= 0.
\end{aligned} \tag{2.5}$$

The explicit forms of the basis functions $\phi_{i,j}$ are provided in Appendix A. An illustration of these Hermite basis functions is shown in Figure 1.

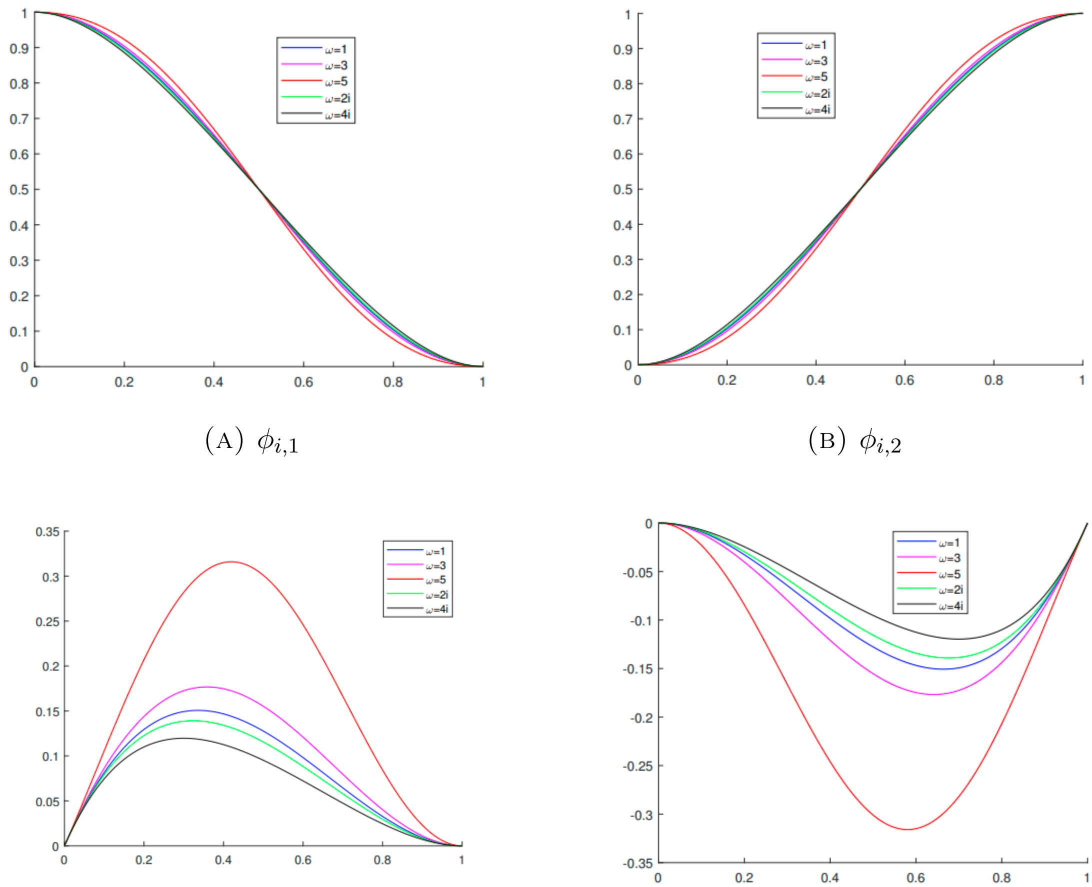

(A) $\phi_{i,1}$ (B) $\phi_{i,2}$

(C) $\phi_{i,3}$ (D) $\phi_{i,4}$

FIGURE 1. Generalized Hermite basis functions $\phi_{i,j}$ for various values of ω, $j = 1$ to 4.

2.3. **Slope Determination via Minimization.** The nodal derivatives m_i are obtained by minimizing the functional

$$I_1(m) = \sum_{i=1}^{n-1} \int_{x_i}^{x_{i+1}} \left(H_i'(x) - L_i'(x)\right)^2 dx, \tag{2.6}$$

where L_i denotes the linear interpolant connecting y_i and y_{i+1}.

Remark 2.2. The full explicit expression of $I_1(m)$ is lengthy and can be found in Appendix B.

2.4. **Asymptotic Expansion and Stability Analysis.** For sufficiently small h, the functional admits the expansion

$$I_1(m) = \sum_{i=1}^{n-1} \Big[C_1(m_i - m_{i+1})^2 + C_2(y_i - y_{i+1})^2 + \mathcal{O}(h^p) \Big], \tag{2.7}$$

where the constants C_1 and C_2 depend on ω and h, with $p > 0$.

The associated linear system for the derivatives m_i is tridiagonal and strictly diagonally dominant for $|\omega|h < \pi$, which guarantees the existence of a unique solution.

2.5. **Tridiagonal System for Slope Minimization.** The minimization of I_1 results in a tridiagonal linear system of the form

$$\begin{pmatrix} \mu & 2v & & & & \\ v & \mu & v & & & \\ & v & \mu & v & & \\ & & \ddots & \ddots & \ddots & \\ & & & v & \mu & v \\ & & & & 2v & \mu \end{pmatrix} \begin{pmatrix} m_1 \\ \vdots \\ m_n \end{pmatrix} = \eta \begin{pmatrix} d_1 \\ d_2 \\ \vdots \\ d_n \end{pmatrix}, \tag{2.8}$$

where the coefficients μ, v, η, and d_i are specified in Appendix C. For detailed expressions of v and η, refer to Appendix D.

The condition ensuring diagonal dominance is

$$\omega\big(\omega h - \sin(\omega h)\big) > 0. \tag{2.9}$$

Lemma 2.3 (Boundedness of the inverse matrix)**.** *Let A denote the coefficient matrix in system* (2.8)*, and assume $|\omega|h < \pi$. Under this assumption, A is strictly diagonally dominant and therefore invertible. Moreover, there exists a constant $C > 0$, independent of the step size h, such that*

$$\|A^{-1}\|_\infty \leq C.$$

Proof. Since the matrix A is strictly diagonally dominant, standard results for tridiagonal matrices (see, e.g., [**?**]) guarantee that A is nonsingular and that its inverse has a bounded ∞-norm. The constant C depends only on ω and the entries of A, and is independent of the step size h provided $|\omega|h < \pi$. □

2.6. **Convergence and Error Analysis.**

Lemma 2.4 (Local Truncation Error)**.** *Let $f \in C^3([a,b])$, and denote by v and η the coefficients appearing in the tridiagonal system* (2.8)*. Then the local truncation errors t_i satisfy*

$$t_i = \left(vh^2 - \frac{\eta h^3}{3}\right) f_i^{(3)} + o(h^2), \quad i = 1, \ldots, n. \tag{2.10}$$

Proof. Expand f and its derivative f' in Taylor series around each node x_i:

$$f(x_{i+1}) = f(x_i) + hf'(x_i) + \frac{h^2}{2}f''(x_i) + \frac{h^3}{6}f^{(3)}(x_i) + o(h^3),$$
$$f(x_{i-1}) = f(x_i) - hf'(x_i) + \frac{h^2}{2}f''(x_i) - \frac{h^3}{6}f^{(3)}(x_i) + o(h^3).$$

Substituting these expansions into the tridiagonal system for m_i and comparing with the exact derivatives $f'(x_i)$ leads to

$$t_i := (AF - C)_i = \left(vh^2 - \frac{\eta h^3}{3}\right) f_i^{(3)} + o(h^2).$$

□

Theorem 2.5 (Accuracy of Slope Approximation)**.** *Let $f \in C^3([a,b])$, and let H denote the generalized Hermite spline whose nodal derivatives minimize the functional I_1. Then the approximation of the slopes satisfies*

$$|m_i - f'(x_i)| = o(h^2), \quad i = 1, \dots, n, \tag{2.11}$$

where the hidden constant depends on $\|f^{(3)}\|_\infty$ and $\|A^{-1}\|_\infty$.

Proof. Denote $F = (f'(x_i))$, $M = (m_i)$, $T = (t_i)$, and let A be the coefficient matrix of the tridiagonal system. We have

$$AM = C, \quad AF = C + T \quad \Rightarrow \quad A(F - M) = T.$$

Since A is strictly diagonally dominant, it is invertible with a bounded inverse:

$$\|F - M\|_\infty \le C\,\|T\|_\infty,$$

where C is the constant from Lemma 2.3. Applying Lemma 2.4, we have $\|T\|_\infty = o(h^2)$, which implies

$$|m_i - f'(x_i)| = o(h^2), \quad i = 1, \dots, n.$$

□

Theorem 2.6 (Interpolation Error for C^4 Functions)**.** *Let $f \in C^4([a,b])$, and let H be the generalized Hermite spline constructed from the data (y_i, m_i). Then the maximum interpolation error satisfies*

$$\|f - H\|_{\infty,[a,b]} = o(h^4), \quad \text{as } h \to 0. \tag{2.12}$$

Proof. On each subinterval $[x_i, x_{i+1}]$, consider the local Hermite polynomial defined by

$$p(x) = f(x_i)\phi_{i,1}(x) + f(x_{i+1})\phi_{i,2}(x) + f'(x_i)\phi_{i,3}(x) + f'(x_{i+1})\phi_{i,4}(x).$$

We then have

$$|H(x) - p(x)| \le |m_i - f'(x_i)|\,\|\phi_{i,3}\|_\infty + |m_{i+1} - f'(x_{i+1})|\,\|\phi_{i,4}\|_\infty = o(h^2),$$

according to Theorem 2.5.

By Taylor's expansion,

$$f(x) - p(x) = \frac{f^{(4)}(\xi)}{24}(x - x_i)^2(x - x_{i+1})^2, \quad \text{for some } \xi \in (x_i, x_{i+1}),$$

which implies $\|f - p\|_{\infty,[x_i,x_{i+1}]} = O(h^4)$.

Combining these bounds, we obtain

$$\|f - H\|_{\infty,[x_i,x_{i+1}]} \le \|f - p\|_\infty + \|p - H\|_\infty = o(h^4).$$

Taking the maximum over all subintervals $[x_i, x_{i+1}]$ completes the proof. □

3. Numerical Examples

To assess the performance of the proposed approach, we compare it with the optimal cubic Hermite interpolation [7] and the optimal quartic interpolation [6]. The generalized Hermite interpolant is capable of exactly reproducing functions in the chosen interpolation space, including trigonometric, hyperbolic, and exponential types, and achieves a quadratic convergence rate $O(h^2)$ (Theorem 1).

The construction of the generalized Hermite interpolant is based on the space

$$\text{span}\{1, x, \cos(\omega x), \sin(\omega x)\} \quad \text{or} \quad \text{span}\{1, x, \cosh(\omega x), \sinh(\omega x)\},$$

depending on whether $\omega \in \mathbb{R}$ or $\omega \in i\mathbb{R}$. The parameter ω is selected to capture the dominant qualitative features of the target function—oscillatory or exponential—while ensuring the stability criterion $|\omega|h < \pi$ is satisfied. In all numerical tests, ω is chosen moderately, well below the upper bound, to maintain stability and prevent ill-conditioning.

We examine the test functions

$$f_1(t) = -\exp(\cos(4\pi t)) - 10\exp(-2t), \qquad f_2(t) = \cosh(t)\exp(\sinh(t)),$$

on the interval $[0, 1]$. The uniform approximation error is defined by

$$\mathcal{E}_h(f, H) := \max_{0 \le i \le n} |f(t_i) - H(t_i)|,$$

where H denotes the generalized Hermite interpolant and t_i are uniformly spaced points. The results reported in Tables 1–3 indicate that the proposed method consistently provides errors that are smaller or comparable to those obtained by Han's approach [7].

		$f(t) = \cos(\pi t)$		
n	Our Method	NCO	Han [7]	NCO
10	0	–	6.23×10^{-1}	–
20	0	–	1.51×10^{-1}	1.93
40	0	–	3.74×10^{-2}	2.01

Table 1. Absolute errors $\mathcal{E}_h(f, H)$.

n	Our Method	NCO	Han [7]	NCO
20	3.16×10^{-3}	–	5.78×10^{-1}	–
40	9.99×10^{-4}	1.66	1.51×10^{-1}	1.93
80	2.79×10^{-4}	1.84	3.57×10^{-2}	2.08
160	7.72×10^{-5}	1.94	8.74×10^{-3}	2.03
320	1.95×10^{-5}	1.98	2.18×10^{-3}	2.00

Table 2. Absolute errors $\mathcal{E}_h(f_1, H)$.

n	Our Method	NCO	Han [7]	NCO
20	2.68×10^{-3}	–	4.32×10^{-1}	–
40	7.31×10^{-4}	1.87	1.13×10^{-1}	1.93
80	1.90×10^{-4}	1.94	2.88×10^{-2}	1.97
160	4.52×10^{-5}	2.07	6.76×10^{-3}	2.09
320	1.12×10^{-5}	2.01	1.69×10^{-3}	2.00

TABLE 3. Absolute errors $\mathcal{E}_h(f_2, H)$.

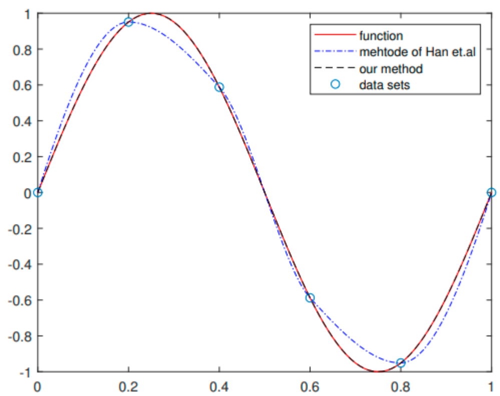

(A) Interpolation of $f(t) = \cos(\pi t)$.

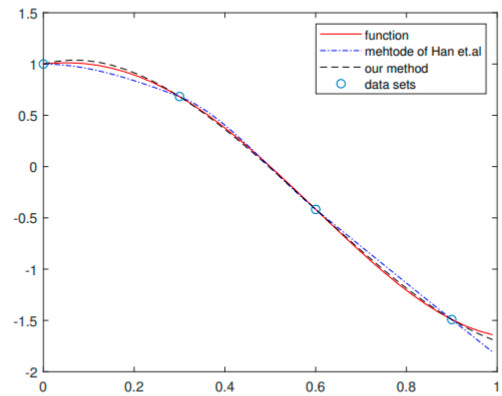

(B) Interpolation of f_1.

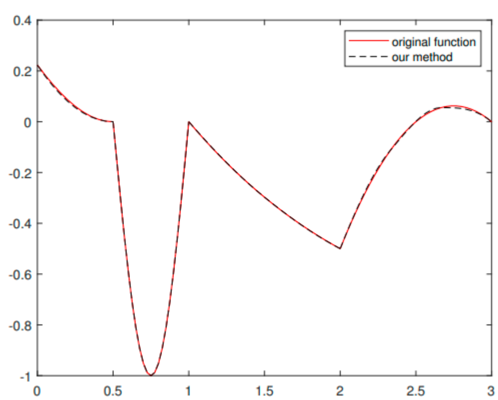

(C) Interpolation of$f_2(t)$ for $n = 25$.

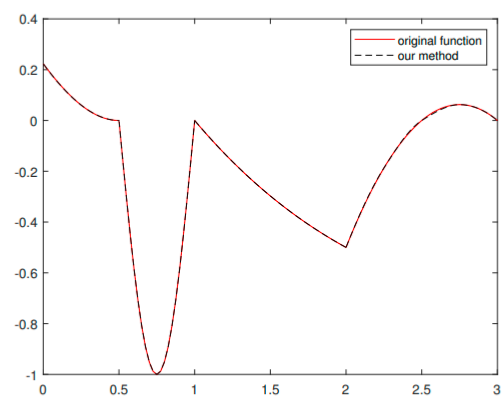

(D) Interpolation of $f_2(t)$ for $n = 35$.

FIGURE 2. Comparison of interpolations: black curves correspond to our method, blue curves to Han [7].

A comprehensive comparison of derivative oscillations for various quartic spline methods is presented in Appendix A.

4. CONCLUSION

In this study, we have proposed an optimal generalized Hermite interpolant that exactly reproduces functions in the linear space $\{1, x, \cos(\omega x), \sin(\omega x)\}$. The free parameters of the interpolant are obtained by minimizing an integral functional that measures the squared deviation of the first derivative of the interpolation error.

The effectiveness of the proposed approach has been validated through several numerical examples. It should be noted that some of the more involved algebraic expressions were derived and simplified using Mathematica.

Future research will aim at extending this framework to comonotone-preserving methods based on generalized spline constructions.

Appendix A. Explicit Basis Functions

The generalized Hermite basis functions $\phi_{i,j}(x)$, $j = 1, \ldots, 4$, are given explicitly by

$$\begin{aligned}
\phi_{i,1}(x) &:= \frac{\omega(x_{i+1}-x)\cos\left(\frac{\omega h}{2}\right) + 2\sin\left(\frac{\omega(x-x_{i+1})}{2}\right)\cos\left(\frac{\omega(x-x_i)}{2}\right)}{\omega h\cos\left(\frac{\omega h}{2}\right) - 2\sin\left(\frac{\omega h}{2}\right)},\\
\phi_{i,2}(x) &:= -\frac{\omega(x_{i}-x)\cos\left(\frac{\omega h}{2}\right) + 2\sin\left(\frac{\omega(x-x_{i})}{2}\right)\cos\left(\frac{\omega(x-x_{i+1})}{2}\right)}{\omega h\cos\left(\frac{\omega h}{2}\right) - 2\sin\left(\frac{\omega h}{2}\right)},\\
\phi_{i,3}(x) &:= -\frac{\csc^2\left(\frac{\omega h}{2}\right)}{2\omega\left(\omega h\cot\frac{\omega h}{2}-2\right)}\Big[\sin(\omega(x-x_i)) - \sin(\omega(x-x_{i+1})) - \sin(\omega h)\\
&\quad - \omega x\cos(\omega h) + \omega x_i(\cos(\omega(x-x_{i+1}))-1) + \omega x_{i+1}(\cos(\omega h)-\cos(\omega(x-x_{i+1}))) + \omega x\Big],\\
\phi_{i,4}(x) &:= \frac{\csc^2\left(\frac{\omega h}{2}\right)}{2\omega\left(\omega h\cot\frac{\omega h}{2}-2\right)}\Big[\sin(\omega(x-x_i)) - \sin(\omega(x-x_{i+1})) - \sin(\omega h)\\
&\quad + \omega x\cos(\omega h) + \omega x_i(\cos(\omega(x-x_{i}))-\cos(\omega h)) - \omega x_{i+1}(\cos(\omega(x-x_{i}))-1) - \omega x\Big].
\end{aligned} \tag{A.1}$$

Appendix B. Explicit Functional I_1

The functional $I_1(m)$ used to select the slopes is given explicitly by

$$\begin{aligned}
I_1(m) = \sum_{i=1}^{n-1} &\frac{h\omega(m_i+m_{i+1})(y_i-y_{i+1})}{2h\omega\left(h\omega\cos\left(\frac{h\omega}{2}\right)-2\sin\left(\frac{h\omega}{2}\right)\right)^2}\Big(h^2\omega^2 + h\omega\sin(h\omega) + 4\cos(h\omega) - 4\Big)\\
&\times\Big[8h^4\omega^3(m_i^2+m_{i+1}^2) + 4\sin(h\omega)\big(h^2\omega^2(m_i^2-3m_im_{i+1}+m_{i+1}^2) + (m_i-m_{i+1})^2\big)\\
&\quad + \sin(2h\omega)\big(h^2\omega^2(m_i^2+m_{i+1}^2) - 2(m_i-m_{i+1})^2\big)\\
&\quad + 4h\omega\cos(h\omega)\big(m_im_{i+1}(h^2\omega^2-6) - m_i^2 - m_{i+1}^2\big)\\
&\quad + 4h\omega(m_i^2+m_{i+1}^2)\cos(2h\omega) + 24h\omega m_im_{i+1}\Big]\,32\omega(y_i-y_{i+1})^2\Big(h^2\omega^2 + h\omega\sin(h\omega) + 4\,\mathrm{co}
\end{aligned} \tag{B.1}$$

Appendix C. Coefficients for Tridiagonal System

The tridiagonal system for slope minimization is

$$\begin{pmatrix} \mu & 2v & & & \\ v & \mu & v & & \\ & v & \mu & v & \\ & & \ddots & \ddots & \ddots \\ & & & v & \mu \end{pmatrix} \begin{pmatrix} m_1 \\ \vdots \\ m_n \end{pmatrix} = \eta \begin{pmatrix} d_1 \\ \vdots \\ d_n \end{pmatrix}. \tag{C.1}$$

The coefficients are defined as

$$v = \text{coefficient linking } m_i \text{ and } m_{i+1} \text{ in } I_1, \tag{C.2}$$
$$\mu = \text{main diagonal coefficient depending on } \omega \text{ and } h, \tag{C.3}$$
$$\eta = \text{scaling factor arising from } I_1, \tag{C.4}$$
$$d_i = \text{function of data differences } y_i - y_{i+1} \text{ and } \omega, h. \tag{C.5}$$

The system is strictly diagonally dominant for $|\omega|h < \pi$, ensuring a unique solution.

Appendix D. Asymptotic Expansions of Coefficients v and η

For small h, the coefficients v and η in the tridiagonal system (2.8) admit the expansions

$$v = \frac{\omega^2}{12}h + \mathcal{O}(h^3), \tag{D.1}$$
$$\eta = \frac{\omega^2}{6}h + \mathcal{O}(h^3). \tag{D.2}$$

These expansions justify the asymptotic estimate

$$vh^2 - \frac{\eta h^3}{3} = \mathcal{O}(h^3),$$

used in Lemma 2.4.

Appendix E. Derivative Oscillations

Finally, we compare derivative oscillations for several quartic spline schemes (S_D, S_C, S_S, S_O). The input data and local derivatives are summarized in Tables 4–5, and the resulting derivative oscillations in Table 6.

i	0	1	2	3	4	5
x_i	0	2	4	6	8	10
y_i	16	20	28	21	24	28

Table 4. Input data.

m_i	m_0	m_1	m_2	m_3	m_4	m_5	I_1
H	-1.0172	3.2407	1.4138	-5.0284	3.1695	-0.8061	388.28
S_D	-1.9689	5.1006	2.5249	-5.5601	5.4596	-1.0811	445.56
S_C	-7.8476	6.9145	7.4880	-10.2250	7.8167	-4.1417	577.23
S_S	-8.7018	7.1929	8.2452	-10.7310	7.9057	-4.5236	587.62
S_O	13.6100	2.7799	15.2700	-12.3610	2.6746	9.6627	460.14

TABLE 5. Local derivatives m_i and functional values I_1.

	H	S_D	S_C	S_S	S_O
$\sqrt{I_1}$	19.705	21.108	24.026	24.241	21.451

TABLE 6. Derivative oscillation.

REFERENCES

1. Akima, H. (1969). *A method of smooth curve fitting* (ESSA Technical Report ERL 101-ITS 73). Washington, DC: U.S. Government Printing Office.
2. Alexandru, M. B. (2021). On the minimal derivative oscillation for deficient quartic splines of Marsden's type. *Journal of Computational and Applied Mathematics, 388*, 113276. https://doi.org/10.1016/j.cam.2020.113276
3. Barrera, D., Eddargani, S., Lamnii, A., & Oraiche, M. (2021). On nonpolynomial monotonicity-preserving C^1 spline interpolation. *Computational and Mathematical Methods, 2021*, e1160. https://doi.org/10.1002/cmm4.1160
4. Bica, A. M. (2012). Fitting data using optimal Hermite type cubic interpolating splines. *Applied Mathematics Letters, 25*, 2047–2051. https://doi.org/10.1016/j.aml.2012.05.010
5. de Boor, C. (1978). *A practical guide to splines*. Springer-Verlag.
6. Fang, M.-E., Ma, W., & Wang, G. (2010). A generalized curve subdivision scheme of arbitrary order with a tension parameter. *Computer Aided Geometric Design, 27*(9), 720–733. https://doi.org/10.1016/j.cagd.2010.09.001
7. Han, X., & Guo, X. (2018). Cubic Hermite interpolation with minimal derivative oscillation. *Journal of Computational and Applied Mathematics, 331*, 82–87. https://doi.org/10.1016/j.cam.2017.08.010
8. Ichida, K., Yoshimoto, F., & Kiyono, T. (1976). Curve fitting by a piecewise cubic polynomial. *Computing, 16*, 329–338. https://doi.org/10.1007/BF02237077
9. Joy, D., & Regala, A. M. (2023). Tension spline approach to singularly perturbed delay differential equations. *Gulf Journal of Mathematics, 15*(2), 166–174. Available at: https://doi.org/10.56947/gjom.v15i2.1314
10. Lamnii, A., Lamnii, M., & Oumellal, F. (2016). A new basis for osculatory interpolation problems and applications. *Applied Mathematics and Computation, 283*, 355–368. https://doi.org/10.1016/j.amc.2016.06.053
11. Lamnii, A., Nour, M. Y., Sbibih, D., & Zidna, A. (2022). Generalized spline quasi-interpolants and applications to numerical analysis. *Journal of Computational and Applied Mathematics*. https://doi.org/10.1016/j.cam.2022.114100
12. Saidi, S., Abbadi, A.,& Tahrichi, M. (2024). Estimating parametric surface areas using spline quasi-interpolants. *Gulf Journal of Mathematics, 18*(1), 54–71. Available at: https://doi.org/10.56947/gjom.v18i1.2370
13. Zhu, Y., & Han, X. (2015). Shape preserving $\mathcal{C}^2$, rational quartic interpolation spline with two parameters. *International Journal of Computer Mathematics, 92*(10), 2160–2177. https://doi.org/10.1080/00207160.2015.1013871

14. Zhu, Y., & Liu, Z. (2019). A class of trigonometric Bernstein-type basis functions with four shape parameters. *Mathematical Problems in Engineering, 2019*, 16. https://doi.org/10.1155/2019/9026187

[1*] University Mohamed First, Laboratory LANO, Faculty of Science Oujda, Oujda, Morocco

Email address: chaimae.mouhoub.d24@ump.ac.ma; https://orcid.org/0009-0007-6209-5307

[2] Université de Tours, LIFAT EA 6300, Tours, France

Email address: mohamedyassir.nour@gmail.com; https://orcid.org/0000-0003-3740-7552